Genomic Effects of IFN-β in Multiple Sclerosis Patients[1]

Bianca Weinstock-Guttman,* Darlene Badgett,† Kara Patrick,* Laura Hartrich,†‡ Roseane Santos,† Dennis Hall,† Monika Baier,§ Joan Feichter,* and Murali Ramanathan[2]*†

The purpose of this report was to characterize the dynamics of the gene expression cascades induced by an IFN-β-1a treatment regimen in multiple sclerosis patients and to examine the molecular mechanisms potentially capable of causing heterogeneity in response to therapy. In this open-label pharmacodynamic study design, peripheral blood was obtained from eight relapsing-remitting multiple sclerosis patients just before and at 1, 2, 4, 8, 24, 48, 120, and 168 h after i.m. injection of 30 μg of IFN-β-1a. The total RNA was isolated from monocyte-depleted PBL and analyzed using cDNA microarrays containing probes for >4000 known genes. IFN-β-1a treatment resulted in selective, time-dependent effects on multiple genes. The mRNAs for genes implicated in the anti-viral response, e.g., double-stranded RNA-dependent protein kinase, myxovirus resistance proteins 1 and 2, and guanylate binding proteins 1 and 2 were rapidly induced within 1–4 h of IFN-β treatment. The mRNAs for several genes involved in IFN-β signaling, such as IFN-α/β receptor-2 and Stat1, were also increased. The mRNAs for lymphocyte activation markers, such as IFN-induced transmembrane protein 1 (9–27), IFN-induced transmembrane protein 2 (1–8D), β_2-microglobulin, and CD69, were also increased in a time-dependent manner. The findings demonstrate that IFN-β treatment induces specific and time-dependent changes in multiple mRNAs in lymphocytes of multiple sclerosis patients that could provide a framework for rapid monitoring of the response to therapy. ***The Journal of Immunology*****, 2003, 171: 2694–2702.**

Recombinant human IFN-β has emerged as one of the most commonly prescribed forms of therapy for relapsing multiple sclerosis (MS)[3] patients on the basis of several double-blind, placebo-controlled, multicenter trials (1–3).

Treatment with recombinant IFN-β-1a has been shown to slow the accumulation of physical disability in MS, reduce the frequency of relapses, and decrease the accumulation of disease burden and atrophy as evaluated by magnetic resonance imaging. IFN-β was also shown to delay the conversion to clinically definite MS in patients with a first demyelinating event (4, 5).

The effects of IFN-β treatment are complex, and its pharmacodynamics at the genomic level in humans are poorly understood. In MS patients in particular, the benefit associated with IFN-β therapy is difficult to monitor (6, 7), and despite extensive examination of the effects of IFN-β in vitro with techniques such as flow cytometry, ELISA, RT-PCR, and proliferation and adhesion assays, the cellular, molecular, and immune mechanisms mediating the clinical effects of IFN-β in MS are poorly delineated. Patients with relapsing MS respond better to IFN-β treatment than patients with progressive disease. However, relapsing MS patients also exhibit considerable interindividual heterogeneity in their clinical responses to IFN-β therapy. Large phase III studies indicate a 30–40% general clinical benefit, although the response varied among patients. Magnetic resonance imaging data also underscore the heterogeneity of responses to IFN-β therapy in MS patients; ~40% of patients show complete suppression of new gadolinium-enhancing lesions, whereas 20% of patients have <70% suppression (8).

The goal of this study was to characterize the dynamics of the gene expression cascades induced by an IFN-β-1a treatment regimen in MS patients and to examine the molecular mechanisms potentially capable of causing heterogeneity in response to therapy. Our results demonstrate that the IFN-β-1a treatment causes large-scale, time-dependent changes in immunomodulatory gene expression in circulating lymphocytes that can be effectively assessed using the array technique. The gene expression changes are orchestrated with immunological changes at the protein and cellular levels.

Materials and Methods

Study population

With informed consent, peripheral blood anticoagulated with heparin was obtained by venipuncture from eight patients (six women and two men; mean age ± SD, 49.0 ± 11.0 years) with active relapsing remitting MS (Expanded Disability Status Scale range, 1.5–6.5; mean Expanded Disability Status Scale ± SD, 2.9 ± 1.6) who were to receive IFN-β therapy. Patients had not previously received IFN-β and were clinically stable for the preceding 4 wk.

Peripheral blood samples were obtained just before treatment and at 1, 2, 4, 8, 24, 48, 120, and 168 h after a 30-μg dose of i.m. IFN-β-1a (Avonex; Biogen, Cambridge, MA). Patients were administered 30 μg of IFN-β-1a i.m. weekly, and additional samples were obtained before the 3 and 6 mo doses.

Cell analysis

A complete blood count and five-point differential were obtained from a clinical laboratory on Coulter STKS and Max M instruments (Beckman Coulter Clinical Diagnostics, Brea, CA).

RNA isolation

PBMC were rapidly isolated using gradient separation on cell preparation tubes (BD Biosciences, Mountain View, CA). Monocytes were depleted

*Jacobs Neurological Institute, Buffalo General Hospital, Buffalo, NY 14203; Departments of †Pharmaceutical Sciences and ‡Pathology, State University of New York, Buffalo, NY 14260; and §Department of Statistics, The Cooper Institute, Golden, CO 80401

Received for publication March 25, 2003. Accepted for publication June 26, 2003.

The costs of publication of this article were defrayed in part by the payment of page charges. This article must therefore be hereby marked *advertisement* in accordance with 18 U.S.C. Section 1734 solely to indicate this fact.

[1] This work was supported by Grant RG3258A2 from the National Multiple Sclerosis Society. R.S. received scholarship support from CAPES, Ministry of Education, Brazil.

[2] Address correspondence and reprint requests to Dr. Murali Ramanathan, Department of Pharmaceutical Sciences, 543 Cooke, Buffalo, NY 14260. E-mail address: murali@acsu.buffalo.edu

[3] Abbreviations used in this paper: MS, multiple sclerosis; AUEC, area under the effect curve; GBP, guanylate binding protein; IFNAR, IFN-α/β receptor; Jak, Janus kinase; Mx-2, myxovirus (influenza) resistance protein 2; Tyk2, tyrosine kinase 2.

0022-1767/03/$02.00

from the PBMC (plastic adhesion), and total RNA was prepared using the Tri-Reagent method (Molecular Research Center, Cincinnati, OH) (9, 10).

DNA arrays

The GeneFilters GF211 DNA arrays (Research Genetics, Huntsville, AL) were used. This commercially available array contains named human genes (5184 total spots each containing 0.5 ng of an ~1000-base, 3′ end-derived PCR fragment). Each filter contained multiple control total genomic DNA-positive control spots and housekeeping genes. The manufacturer selected certain genes as housekeeping genes because these did not differ in hybridization signal among several different tissues in an analysis performed at the National Institute of Health. However, some of these housekeeping genes are expressed at relatively low levels, while others are expressed at much higher levels. Each housekeeping gene was spotted in duplicate, and there were >4000 known genes in the GF211 array. A complete database of the genes on the filter is available online at ftp://ftp.resgen.com/pub/genefilters/.

The manufacturer's recommended protocols were used (http://www.resgen.com). Five micrograms of total RNA was radioactively labeled with [^{33}P]CTP using reverse transcriptase with oligo(dT) primers. The labeled cDNA from each RNA sample was individually used to probe the GF211 membrane. The membranes were washed, and the bound radioactivity was visualized using a Cyclone phosphorimager (Packard Instrument, Meriden, CT). The membranes were rehybridized with cDNAs after stripping. In pilot experiments the stripping time (1.5 h) was optimized by phosphorimaging to minimize residual radioactivity, a potential source of bias.

Data analysis

The phosphorimager-generated images were imported directly into the Pathways 4.0 software program (Research Genetics), aligned, gridded, and quantitated. The Pathways software program allows normalization relative to the set of housekeeping genes or global normalization relative to all spots on the array. Because treatments can often cause changes in the expression of housekeeping genes, the global normalization option was selected, i.e., each of the filters were normalized using the intensity from all spots on the GF211 GeneFilter DNA array and for intensity ranges; this results in datasets in which the average normalized intensity across all spots is 1. The normalized intensity data were treated as expression levels for the genes and exported to an Excel spreadsheet (Microsoft, Bellevue, WA).

For statistical analysis, the relative expression level for each gene in a given patient was obtained as the fold change in the normalized intensity value relative to the expression level of the gene in the pretreatment sample of the patient. The figures show the average value of the relative expression values across the available patients (eight patients for Figs. 1–3, individual patients for Fig. 4, and seven patients for Fig. 6), and the error bars are the SDs.

Statistical analysis was performed using the Excel, SPSS 6.1 (SPSS, Chicago, IL) and SAS (SAS Institute, Research Triangle Park, NC) software programs. Repeated measures analysis with a mixed effect model and linear contrasts was employed for statistical analysis of the time-course data for each gene of interest. The PROC MIXED procedure in the SAS statistical program (SAS Institute) was used. Nonparametric rank correlation analysis was performed using SPSS 6.1 (SPSS, Chicago, IL).

The Bayesian approach was used for cluster analysis because of its ability to account for the time dependency of the gene expression data from the pharmacodynamic study design (11). The gene expression time-series data were natural logarithm-transformed and represented as autoregressive process of Markov order 1, i.e., the expression at each time point is conditionally independent of the past if the expression at the preceding time point is given. The approach initially assumes that all clusters are equally likely and then uses the marginal likelihood as a similarity measure in an agglomerative procedure to identify the most probable set of clusters. The prior precision and the γ value were set at 1 and 0, respectively. The Euclidean distance was used to guide the search process.

The trapezoidal rule was used for area under the effect curve calculations. The data for each patient were normalized to the corresponding pretreatment values at this step.

Bioinformatics

The abbreviations used in the text and the Unigene identifiers for many of the genes discussed in *Results* are shown in Table I. In addition to the genes in Table I, the expression of the following genes associated with IFN-β signaling were analyzed: the IFN (α, β, and ω) receptor 1 (IFNAR1, Hs.1513), the IFN (α, β, and ω) receptor 2 (IFNAR2, Hs.86958), Janus kinase 1 (Jak1; Hs.50651), tyrosine kinase 2 (Tyk2; Hs.75516), and 48-kDa IFN-stimulated transcription factor 3γ (p48, Hs. 1706). The following lymphocyte activation genes were also investigated: early T cell activation Ag (CD69, Hs.82401), IFN-induced transmembrane protein 1 (9–27, Hs.146360), IFN-induced transmembrane protein 2 (1–8D, Hs.174195), IFN-induced transmembrane protein 3 (1–8U, Hs.182241), and β_2-microglobulin (Hs.75415). The 9–27, 1–8D, and 1–8U genes are involved in the transduction of antiproliferative and homotypic adhesion signals (12, 13).

Real-time quantitative PCR measurements

Real-time quantitative PCR (real-time PCR) was used to confirm the key results from the array experiments. The RNA samples from the pretreatment and 2, 8, and 24 h points for four patients (a subset of the eight patients examined using arrays) were analyzed for five genes: β-actin, myxovirus resistance protein 1, myxovirus resistance protein 2, Stat1, and β_2-microglobulin.

Table I. *The set of IFN-stimulated genes used for Bayesian cluster analysis*

Cluster	Unigene ID	Abbreviation	Gene Name
1	*Hs.833*		IFN-stimulated protein, 15 kDa
1	*Hs.183487*		IFN-stimulated gene (20 kDa)
1	*Hs.82030*		Tryptophanyl-tRNA synthetase
1	*Hs.241510*		IFN-induced protein 41, 30 kDa
1	*Hs.146360*	9–27	IFN-induced transmembrane protein 1 (9–27)
1	*Hs.1279*		Complement component 1, r subcomponent
1	*Hs.21486*	Stat-1	Stat-1, 91 kDa
1	*Hs.62661*	GBP-1	GBP-1, IFN-inducible, 67 kDa
1	*Hs.20315*		IFN-induced protein 56
1	*Hs.274382*	PRKR	Protein kinase, IFN-inducible dsRNA dependent
1	*Hs.926*	Mx2	Mx2
2	*Hs.79322*		Glutaminyl-tRNA synthetase
2	*Hs.278613*		IFN-α-inducible protein 27
2	*Hs.86958*	IFNAR2	IFN (α, β, and ω) receptor 2
2	*Hs.76391*	Mx1	Mx1
2	*Hs.80645*		IFN regulatory factor 1
2	*Hs.174195*	1–8D	IFN-induced transmembrane protein 2 (1–8D)
2	*Hs.171862*	GBP-2	GBP-2, IFN-inducible
2	*Hs.155530*		IFN-γ-inducible protein 16
2	*Hs.77367*		Monokine induced by IFN-γ
2	*Hs.83795*	IRF-2	IFN regulatory factor 2
2	*Hs.277477*	HLA-C	MHC, class I, C
2	*Hs.14623*		IFN-γ-inducible protein 30
2	*Hs.75415*		β_2-Microglobulin

Real-time quantitative PCR measurements were made on an MX4000 Multiplex Quantitative PCR System (Stratagene, La Jolla, CA) using the TaqMan probe assay. The primer pairs and TaqMan probes, which were 5′ labeled with a 6-carboxyfluorescein (FAM) reporter and 3′ labeled with a quencher, were custom ordered from Applied Biosystems (Assay on Demand, Foster City, CA).

The total RNA (200 ng) from each sample was reverse transcribed to cDNA using the Superscript First Strand Synthesis System (Invitrogen, Carlsbad, CA) with oligo$(dT)_{12-18}$ primers according to the manufacturer's instructions. Briefly, the following steps and reaction conditions were involved in cDNA preparation: denaturation at 65°C for 5 min, followed by annealing on ice; RT at 42° C for 50 min; termination at 70° C for 15 min, followed by chilling on ice; and RNA template digestion by RNase H treatment at 37°C for 20 min.

Sequence-verified EST IMAGE clones containing β-actin, myxovirus resistance protein 1, myxovirus resistance protein 2, Stat1, and β_2-microglobulin genes were obtained as bacterial cultures from American Type Culture Collection (Manassas, VA) and processed to obtain standards for absolute quantitation. Plasmids were purified from overnight bacterial cultures in antibiotic-containing medium using Wizard Plus miniprep system (Promega, Madison, WI). Plasmid DNA concentration was quantitated by measuring Hoechst 33258 fluorescence on a DynaQuant 200 fluorometer (Amersham Pharmacia Biotech, Piscataway, NJ). Copy concentrations in the stocks were calculated using the molecular weights of the plasmids.

Real-time PCR reaction for cDNA samples, serial dilutions of the standard plasmids over a 10^6-fold range of copy number, and nontemplate controls were performed in a 96-well microtiter plate format on a MX4000 Multiplex Quantitative PCR System (Stratagene, La Jolla, CA). Briefly, each reaction (50 μl total volume) contained 25 μl of 2× TaqMan Universal PCR Master Mix (PE Applied Biosystems), 2.5 μl of 20× Assay on Demand Gene Specific Mix containing the TaqMan probe and primers, and 22.5 μl of the cDNA sample (corresponding to 40 ng of RNA), standard plasmid, or nontemplate control in sufficient RNase-free water. The thermal cycler conditions for all five genes were: initial set up at 95°C for 10 min and 40 amplification cycles, each consisting of denaturation at 95°C for 15 s, followed by annealing and extension at 60°C for 1 min. The instrument measures the fluorescent signal generated by the release of the FAM label on TaqMan probe during each PCR cycle via 5′-3′ endonuclease activity of AmpliTaq Gold DNA polymerase. Each well was screened for fluorescence during each annealing/extension cycle, and three replicate measurements were made. The cycle threshold, defined as the cycle at which fluorescence intensity exceeds 10 times the SD of the baseline fluorescence, was computed for each well from the individual fluorescence plots using computer software (14). The cycle threshold values for the serial dilutions of standards were plotted against the logarithm of copy number values to generate a standard curve for quantitation of each mRNA of interest. The correlation coefficient of the standard curves was $r = 0.98$ or greater. The copy number for each gene was computed using the regression equation, and additionally, the data for each sample were normalized using the level of β-actin mRNA.

Immunophenotyping analysis

Immunophenotyping results were available for seven of the eight patients. For two of the seven patients, data were available only at the baseline and 1, 2, 4, 8, 24, and 48 h points.

Peripheral blood anticoagulated with heparin was used for staining. The four-color Ab conjugate panel (FITC-conjugated anti-CD3, PE-conjugated anti-CD56, PC tandem-conjugated anti-CD19, and allophycocyanin-conjugated anti-CD69) was capable of delineating activated T, B, and NK cells when used in conjunction with appropriate isotype controls. The NK cells were defined as cells expressing the CD56 marker, and the T cells were defined as those expressing the CD3 marker. The expression of CD69 was used to identify activated cells.

For staining, 2.5 ml of peripheral blood was washed once with 12.5 ml of cold PBS containing 0.1% heparin (Life Technologies, Grand Island, NY). After a second wash with 15 ml of PBS, purified mouse IgG (Caltag Laboratories, San Francisco, CA) was added to the cell suspension at a concentration of 200 μg/ml and incubated at 4°C for 10 min to block FcR binding.

Aliquots of cell suspension (50 μl) were incubated with 30 μl of Ab panel for 15 min at 4°C. In addition, a control tube treated with ethidium monoazide (5 μl of 5 μg/ml for 10 min under fluorescent light; Molecular Probes, Eugene, OR) was also prepared to allow dead cell exclusion during analysis. The erythrocytes were lysed with 3 ml of lysing solution (8.26 g/L ammonium chloride, 1 g/L potassium bicarbonate, and 0.027 g/L of tetrasodium EDTA in twice-distilled water prepared fresh daily). The tubes were centrifuged at 1500 × g for 3 min, and the cell pellet was washed with cold PBS. The stained cells were fixed in 200 μl of 2% ultra-pure formaldehyde in PBS (Polysciences, Warrington, PA) and kept at 4°C in the dark before analysis on a FACSCalibur flow cytometer (BD Biosciences, San Jose, CA).

Data from the cytometer were analyzed using WinList software (Verity Software, Topsham, ME). The data were exported to an Excel spreadsheet (Microsoft) for normalization before statistical analysis. The cell number data for each subset were calculated from the flow cytometry-derived percentages and the white blood cell count.

Plasma β_2-microglobulin measurements

The level of β_2-microglobulin protein in plasma was measured using a commercially available ELISA kit (ICN Pharmaceuticals, Orangeburg, NJ) according to the manufacturer's instructions.

Results

Pharmacodynamics of IFN-β-1a-induced antiviral genes

The antiviral actions of IFN-β are one of its signature effects and have been well characterized in vitro. Fig. 1*A* shows the dynamics

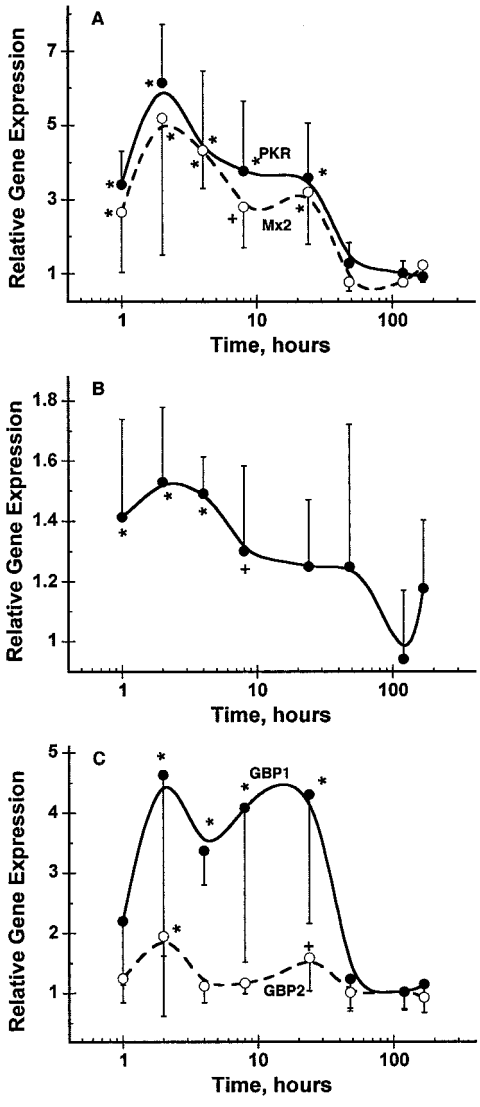

FIGURE 1. The dynamics of antiviral genes induced by IFN-β-1a administration. *A*, Double-stranded RNA-dependent protein kinase (●) and Mx2 (○); *B*, Mx1; *C*, GBP-1 (●) and GBP-2 (○). The *y*-axis is the average relative expression level in the eight patients; the error bars are SDs across the eight patients. The relative expression value for each gene in a given patient was obtained by normalizing to the expression levels in the pretreatment sample for that gene and patient. The lines are a smooth curve to the data. +, $p \leq 0.05$; ∗, $p \leq 0.005$.

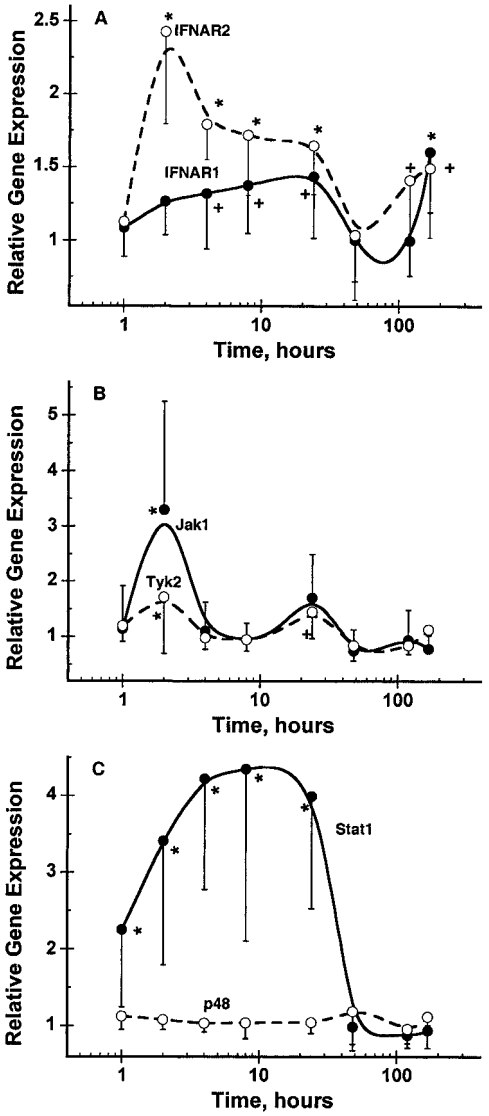

FIGURE 2. The dynamics of genes involved in IFN-β signaling. *A*, Dynamics of IFNAR1 (●) and IFNAR2 (○); *B*, dynamics of Jak1 (●) and Tyk2 (○) expression; *C*, expression of Stat1 (●) and p48 (○). The *y*-axis is the average relative expression level in the eight patients; the error bars are SDs across the eight patients. The relative expression level for each gene in a given patient was obtained as the fold change in the normalized intensity value relative to the expression level of the gene in the pretreatment sample of the patient. The lines are a smooth curve to the data. +, $p \leq 0.05$; ∗, $p \leq 0.005$.

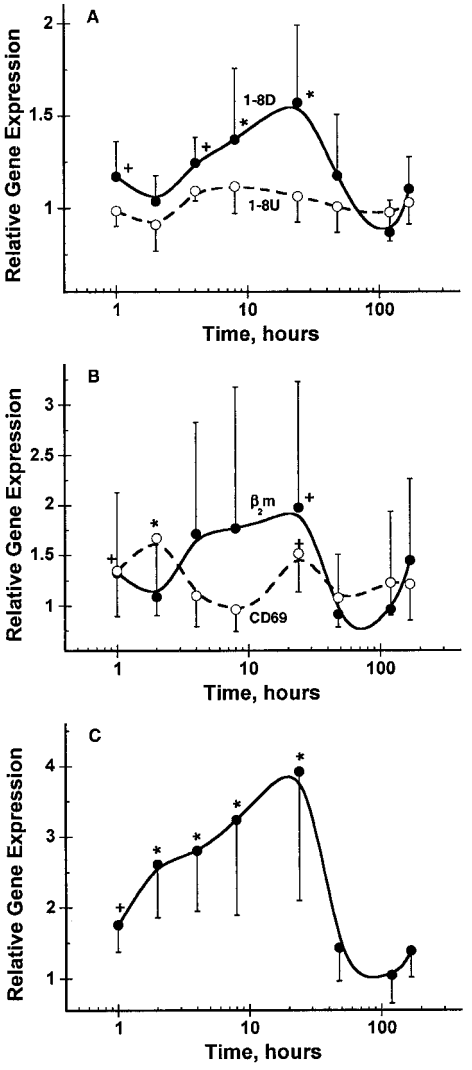

FIGURE 3. The dynamics of genes involved in lymphocyte activation. *A*, Dynamics of 1–8D (●) and 1–8U (○); *B*, β_2-microglobulin (●) and CD69 (○); *C*, 9–27 expression. The *y*-axis is the average relative expression levels in the eight patients; the error bars are SDs across the eight patients. The relative expression level for each gene in a given patient was obtained as the fold change in the normalized intensity value relative to the expression level of the gene in the pretreatment sample of the patient. The lines are a smooth curve to the data. +, $p \leq 0.05$; ∗, $p \leq 0.005$.

of IFN-inducible dsRNA-dependent protein kinase, myxovirus (influenza) resistance protein 2 (Mx2; also known as MxB in humans), Fig. 1*B* shows the expression of Mx1 (also known as MxA in humans, the homologue of murine IFN-inducible protein p78), and Fig. 1*C* shows IFN-inducible guanylate binding protein 1 (GBP-1; 67 kDa) and GBP-2.

The mRNAs for all the antiviral genes shown in Fig. 1 were rapidly induced and reached peak values at 2 h. The mean fold induction values (±SD) at the peak were 6.14 ± 1.44 for mRNAs of IFN-inducible dsRNA-dependent protein kinase, 5.20 ± 3.68 for Mx2, and 4.63 ± 3.01 for GBP-1. The peak mean fold induction values for mRNAs of Mx1 and GBP-2 were lower in comparison (1.53 ± .247 and 1.95 ± 1.33, respectively).

Pharmacodynamics of genes in the Jak-Stat pathway

The transcriptional actions of IFN-β are mediated by the Stat family of transcription factors (15). The IFN-α/β receptor has two subunits, IFNAR1 and IFNAR2c, and IFN-α/β binding results in mutual cross-phosphorylations of Tyk2, an IFNAR1-associated kinase, and Jak1, an IFNAR2c-associated kinase (16). These kinases sequentially phosphorylate IFNAR1, Stat2, and Stat1 at critical tyrosines, causing the release of the Stat1-Stat2 heterodimer from the receptor complex. The heterodimer binds p48 to constitute ISGF3, which translocates to the nucleus, and binds to and modulates transcription from genes containing the IFN-stimulated response element.

We examined genes in the Jak-Stat pathway because they are critical and proximal to the actions of IFN-β. Fig. 2*A* shows the dynamics of IFNAR1 and IFNAR2, Fig. 2*B* shows the dynamics of Jak1 and Tyk2, and Fig. 2*C* shows Stat1 and p48. The mRNAs for

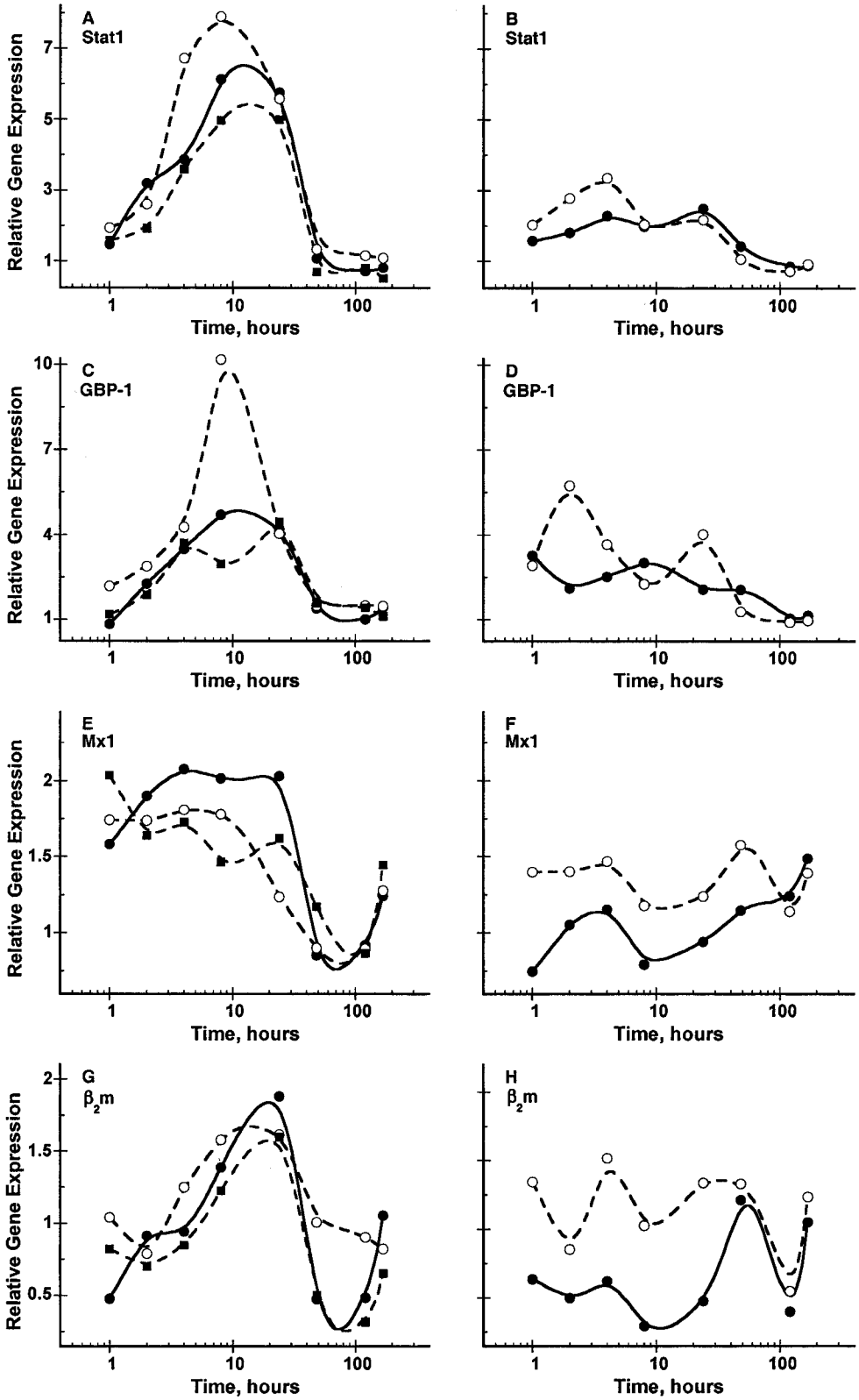

FIGURE 4. Interindividual variations in gene expression dynamics for five representative patients. Four genes were selected: Stat1 (*top row*, *A* and *B*), GBP-1 (*C* and *D*), Mx1 (*E* and *F*), and β_2-microglobulin (β_2m; *G* and *H*). The dynamics of the three patients in the *left panel* (*A*, *C*, *E*, and *G*) are different from those of the two patients in the *right panel* (*B*, *D*, *F*, and *H*). The expression levels on the *y*-axis are relative expression values, obtained as the fold change in the normalized intensity value relative to the expression level of the gene in the pretreatment sample of the patient. The *y*-axis scales for both panels are matched.

IFNAR2 and Stat1 were prominently induced after IFN-β treatment; IFNAR2 reached a peak fold induction level (mean $\pm$ SD) of 2.43 $\pm$ 0.63 at the 2 h point, while Stat1 mRNA reached peak fold induction value of 4.35 $\pm$ 2.25 at the 8 h point. The expression of Jak1 and Tyk2 mRNAs showed peak fold inductions of 3.30 $\pm$ 1.95 and 1.72 $\pm$ 1.02, respectively, at the 2 h point, and there was a systematic increasing trend toward increased IFNAR1 levels. The expression of p48 was not significantly increased.

Dynamics of immune activation marker mRNAs after IFN-β-1a administration

Fig. 3 shows the time dependence of lymphocyte activation markers after administration of IFN-β-1a; Fig. 3A shows the dynamics of 1–8D and 1–8U, Fig. 3B shows β_2-microglobulin and CD69, and Fig. 3C shows 9–27 expression. Except for CD69, these genes have been previously reported to be IFN inducible (15, 17, 18).

The mRNA for the 9–27 gene was prominently increased, and a peak value 3.93-fold greater than baseline was reached at 24 h. The maximal fold changes from baseline for 1–8D, β_2-microglobulin, and CD69 mRNAs were 1.5- to 2-fold. In these experiments the 1–8U gene, which is the paralog of 1–8D, was not significantly modulated by IFN-β-1a.

Interindividual variations in gene expression responses

The pharmacodynamic expression profiles of four IFN-β-induced genes, Stat1, GBP-1, Mx1, and β_2-microglobulin, for five patients are summarized in Fig. 4. Fig. 4 appears to indicate two distinct patterns of responses to the first dose of IFN-β: the patients in the *right panels* (Fig. 4, *B*, *D*, *F*, and *H*) had lower levels of induction and less orderly profiles than the patients in the *left panels*. The profiles of the remaining three patients (data not shown) were generally similar to those in the *left panels* of Fig. 4, although, one of the three patients appeared to respond earlier for several genes. The clinical significance of these interindividual profile differences is not understood at this time. However, these patients are currently being monitored clinically and by quantitative neuroimaging measures, and the associations between these pharmacodynamic findings and the long term response to therapy will be assessed in the future.

Bayesian clustering

We selected 24 genes (Table I) that were known to be IFN-stimulated from work by other laboratories for Bayesian clustering analysis (15, 18). The clustering analysis identified two clusters that differed primarily in the extent of the fold induction. The cluster members are shown in Table I, and the detailed time profiles are

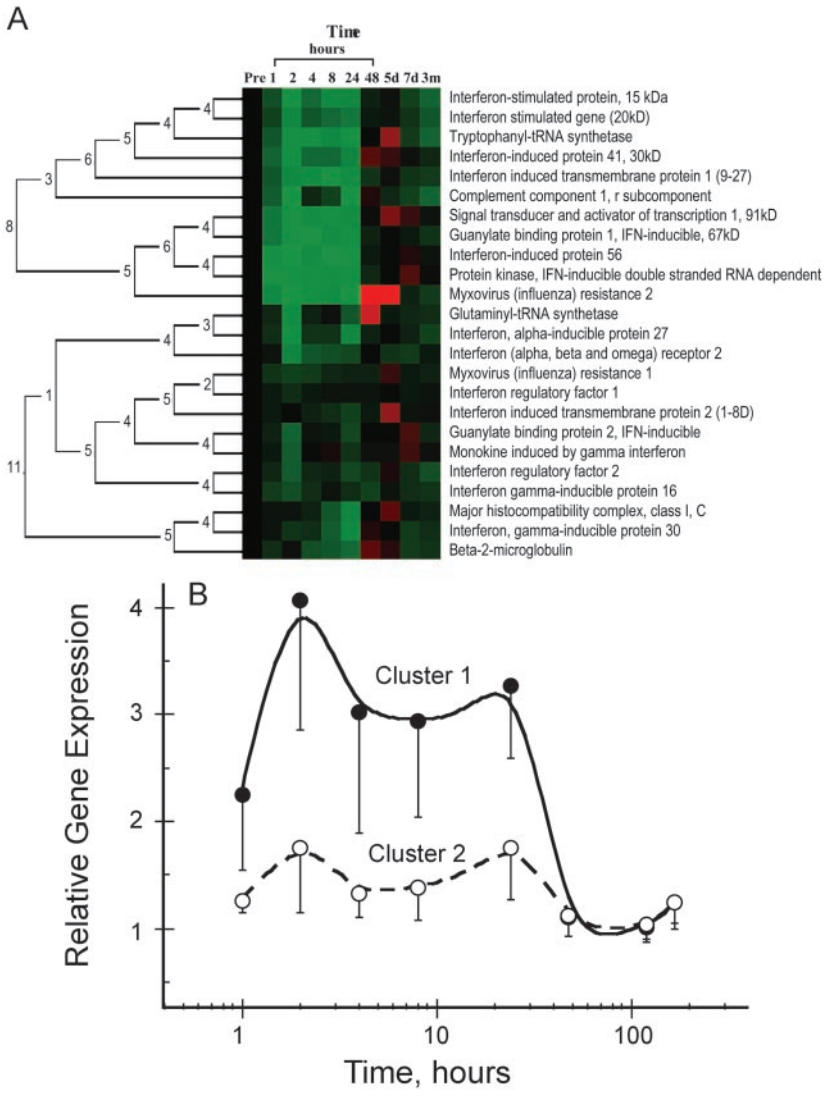

FIGURE 5. *A*, Summary of the hierarchical structure of the clustering model and the dendrogram obtained from Bayesian cluster analysis using the software program CAGED. The *far left side* of *A* shows the tree or dendrogram structure of each cluster. The numbers at the branch points of the tree are the Bayes factor for each merging on a logarithmic scale. The average relative expression level for each gene at the each time point is a square in the heat plot; each column represents a time point (pretreatment; 1, 2, 4, 8, 24, and 48 h; 5 days; 120 h and 7 days; or 168 h and 3 mo), and each row corresponds to the gene described in the *far right* column. The intensity of each color is proportional to the distance of each value from the cut-point, which in this case was set at zero. Intensities are transformed on a natural logarithmic scale. *B*, The mean profile corresponding to all genes in each cluster at a given time point. The error bars are the SDs, and the lines are a smooth curve through the data.

shown in Fig. 5*B*. The time course indicates that changes in mRNA levels of IFN-stimulated genes in vivo in lymphocytes occurs as early as 1–2 h after treatment, and mRNA-based end points could potentially provide early sentinel markers for assessing therapeutic efficacy. The quantitative interrelationships between genes are summarized in Fig. 5*A* as a dendrogram and as a heat plot. The dendrogram also contains the Bayes factor for each merger on a logarithmic scale. The Bayes factor is the ratio of the posterior probabilities of the merged and unmerged or separated clustering models; it indicates how many times more probable is the merged clustering model than the unmerged or separated clustering model.

We also directly assessed the correlation between the time profiles of all 24 genes (data not shown) using the Pearson correlation matrix. The Pearson correlation coefficients were generally higher for gene profiles within Cluster 1 than within Cluster 2. Interestingly, the time profiles for four genes, 1–8D, MHC class C, β_2-microglobulin, and IFN-γ inducible protein 30 (a lysosomal thiol reductase that may be involved in MHC class II-restricted Ag processing; its absence in melanomas affect T cell recognition of immunodominant epitopes), were poorly correlated with other profiles in their cluster, but highly correlated with each other (Pearson correlation coefficients ranged from 0.83–0.975) and with 9–27. These genes are involved in the lymphocyte activation or Ag presentation/recognition, and their orchestration by IFN-β-1a may differ from that of the antiviral genes.

Interestingly, when the columns corresponding to 7 day and 3 mo samples on the heat plot (Fig. 5*A*) were compared, several genes were modulated. This is consistent with the possibility that longer term immunomodulatory processes are also involved in IFN-β-1a action.

Confirmation by real-time PCR

We were initially surprised to observe the maximum up-regulation of Mx1 mRNA at the 2 h point, because Mx1 has previously been evaluated as a surrogate marker for assessing IFN-β responses in MS patients, but usually at the 12 h point (19).

We used real-time PCR to measure the expression of Mx1, Mx2, Stat1β_2-microglobulin,and β-actin mRNA in total RNA samples from four patients at the pretreatment and 2, 8, and 24 h points. The expression level of each mRNA was normalized using the level of β-actin mRNA at the same time point.

In the real-time PCR, the maximum levels of Mx1 and Mx2 were observed in the 2 h samples, maximum levels of Stat1 were observed in the 8 h sample, and the β_2-microglobulin mRNA profile continued to indicate an increasing trend in the 24 h samples (data not shown). Thus, the overall patterns of gene expression revealed by real-time PCR results are similar to those obtained using arrays.

Correlation between CD69 mRNA dynamics and cellular activation

To examine the relevance of array-based mRNA level measurements to downstream events leading to immunomodulation, we examined the correlation between CD69 mRNA level (obtained from array measurements) to the number of NK cells and T cells expressing cell surface CD69 obtained from immunophenotyping ($CD69^+$, $CD3^+$ plus $CD69^+$, $CD56^+$ cells). Operationally, NK cells were defined as cells expressing the CD56 marker, and T cells as those expressing the CD3 marker.

Fig. 6*A* compares the time profiles for CD69 mRNA (●), the numbers of NK cells expressing CD69 (■), and the number of NK and T cells expressing CD69 (□). Fig. 6*A* visually demonstrates that the increases in CD69 mRNA levels were closely associated with changes in the appearance of CD69 expressing NK and T cells in peripheral blood. Fig. 6*B* further assesses the strength of the association by plotting the mean area under the effect curve (AUEC) for CD69 mRNA against the mean AUEC for cell surface CD69-expressing T and NK cells. The correlation between CD69 mRNA AUEC and AUEC for cell surface CD69-expressing T and NK cells was statistically significant; the nonparametric Spearman rank correlation coefficient r_s was 0.967 ($p < 0.001$).

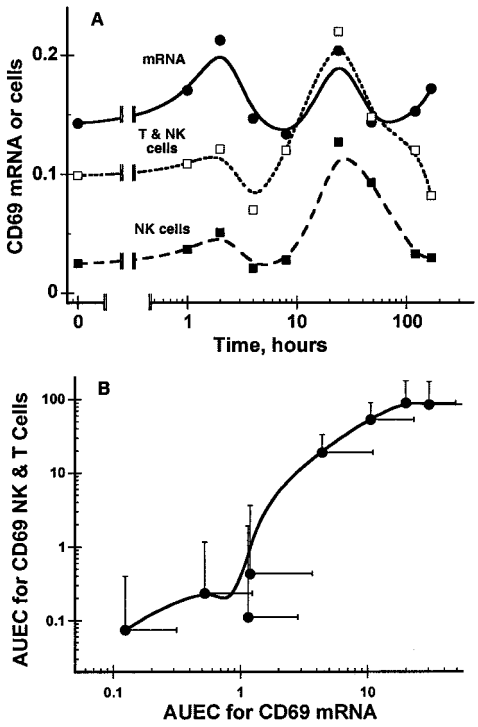

FIGURE 6. A, Comparison of average CD69 expression at the mRNA level (●) from monocyte-depleted lymphocytes to the average number of cell surface CD69-positive NK cells ($CD69^+$, $CD56^+$ cells; ■, closely dashed line) and the average number of cell surface CD69-positive T and NK cells ($CD69^+$, $CD3^+$ plus $CD69^+$, $CD56^+$ cells; □, dashed line) in peripheral blood as measured by flow cytometry. The average mRNA levels are expressed in arbitrary normalized intensity units, and the average CD69-positive cells are in thousands of cells per microliter. *B,* Plot of the average area under the effect curve for CD69 mRNA against the average area under the effect curve for cell surface CD69-positive T and NK cells. The data for each patient were normalized to the pretreatment value. The error bars are the SDs, and the lines are a smooth curve through the data.

IFN-β treatment results in functional orchestration of transcriptional, post-transcriptional, and immunological events in patients

The time profiles of NK cell activation and β_2-microglobulin protein levels in plasma were compared to determine whether IFN-β results in orchestration of functionally related immunological processes. The β_2-microglobulin protein protects against NK cell-mediated cytotoxicity and is known to be IFN-β induced via transcription in vivo. The peak levels of β_2-microglobulin protein occur at 24–48 h, and the profiles are very similar to those of activated NK cells (Fig. 7). The levels of β_2-microglobulin mRNA, which peak between the 8 and 24 h points and decline by the 48 h point (see Fig. 3*B*), precede the peak for β_2-microglobulin in plasma. These results demonstrate that the transcription and post-transcriptional processes related to the β_2-microglobulin gene are coordinately regulated with immunological processes related to NK cell activation.

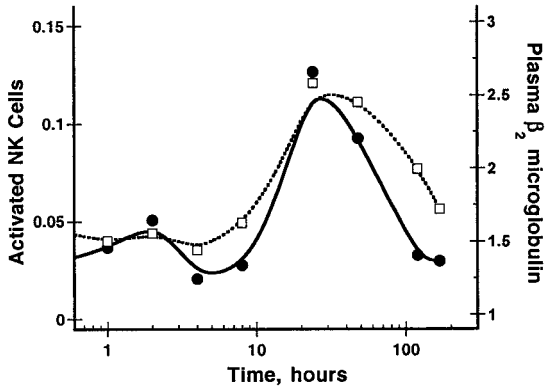

FIGURE 7. Comparison of the dynamics of activated NK cells (●, solid line, *left* axis) to the expression of β_2-microglobulin protein in plasma (□, dashed line, *right* axis). The cell numbers are in units of thousands of cells per microliter, and the plasma β_2-microglobulin concentration is expressed as micrograms per milliliter. The lines are smooth lines through the data.

Discussion

In this report we have investigated the genomic effects of IFN-β-1a treatment on lymphocytes in the peripheral blood of MS patients. The results demonstrate a rich, orchestrated tapestry of mRNA level changes that support functionally related post-transcriptional and immune events.

The pharmacodynamic profiles indicate that measurable changes in mRNA expression occur within 1–4 h of i.m. administration. These mRNA changes occur much earlier than the changes in neopterin, β_2-microglobulin, and Mx protein levels and cellular 2′-5′ oligoadenylate activity, which have previously been used as markers (20–22). To our knowledge this is the first report of the expression profiling of a clinically relevant drug in a pharmacodynamic study design in patients.

Several investigators have recently used arrays to profile lesions from autopsy MS brains (23–26). Because the overall picture of the disease process that emerges from these array studies reflects active migration of lymphocytes cells into lesions, we focused on PBL.

Wandinger et al. (27) treated PBMC from three MS patients with IFN-β-1b (100 and 1000 IU/ml) in vitro, examined the gene expression profiles at 6 and 24 h, and reported a complex repertoire of responses that included the expected anti-inflammatory effects as well as proinflammatory responses.

Satoh and Kuroda (28) compared the effects of IFN-β and IFN-γ treatment on astrocytes and found that Stat-1, HLA-C, and IFN regulatory factor-7 were strongly induced by IFN-β. In our array experiments, peak IFN regulatory factor-7 mRNA levels were increased 5-fold relative to pretreatment levels (data not shown), and our results for Stat-1 and HLA-C are consistently similar to those reported by Satoh and Kuroda (28). These findings suggest that mRNA changes in lymphocytes may mirror some of the treatment-mediated changes that occur in astrocytes.

Array-based methodologies yield large datasets, and there are no standardized approaches to data analysis. The cellular responses to the IFNs are also complex and may encompass >300–500 genes (15, 18), which represents ~0.5% of the genes in the human genome (29). Given the complexity of the technique and the biological system, we opted for a functional approach to analysis and focused on known IFN-stimulated genes and the IFN-signaling pathway. We selected a subset of IFN-stimulated genes previously found to be IFN sensitive in the databases provided previously (15, 17, 18). Further analysis of the other genes is underway.

Our arrays are commercially obtained, use radioactive readouts, and assess the expression levels of ~4000 mRNAs on a filter that contains named human genes. Unlike arrays containing a limited number of genes restricted to a single mechanistic pathway, this filter contains genes with a breadth of functions. This approach makes efficient use of scarce, patient-derived material, and it allows pathway interactions as well as the unexpected effects of treatment to be assessed. The expression levels of genes in specific pathways can be obtained from this filter using software macros. Additionally, in this study total RNA from monocyte-depleted peripheral blood cells was used, and we opted to separate the various cell types, because IFN-β treatment also causes selective trafficking of different cell types in and out of peripheral blood (30). Selective or differential cell trafficking can potentially introduce additional variability in array data because it is difficult to separate the gene expression level changes that are caused by changes in the transcription rates from those caused by changes in cell numbers. Therefore, the genomic changes in monocytes, which may be an important target cell type for IFN-β immunomodulation, were not measured (31–34).

MS is a polygenetic disease that involves the interplay of multiple genes, gene-gene interactions, and post-transcriptional regulatory mechanisms (35, 36), and these factors may contribute to considerable clinical variability in disease presentation and in treatment effects. Because they provide multiplexed measurements of thousands of mRNAs, arrays hold the promise of providing insights into the net result of multiple genes and into gene-gene interactions (37–39). The therapeutic/pharmacological effects of IFN-β are primarily the indirect result of gene transcription effects, and our results support the premise that gene expression profiling for IFN-β treatment effects may lead to improved, and possibly individualized, treatment regimens.

References

1. IFNB Multiple Sclerosis Study Group. 1993. Interferon β-1b is effective in relapsing-remitting multiple sclerosis. I. Clinical results of a multicenter, randomized, double-blind, placebo-controlled trial. *Neurology 43:655.*
2. PRISMS (Prevention of Relapses and Disability by Interferon β-1a Subcutaneously in Multiple Sclerosis) Study Group. 1998. Randomized double-blind placebo-controlled study of interferon β-1a in relapsing/remitting multiple sclerosis. *Lancet 352:1498.*
3. Jacobs, L. D., D. L. Cookfair, R. A. Rudick, R. M. Herndon, J. R. Richert, A. M. Salazar, J. S. Fischer, D. E. Goodkin, C. V. Granger, J. H. Simon, et al. 1996. Intramuscular interferon β-1a for disease progression in relapsing multiple sclerosis: The Multiple Sclerosis Collaborative Research Group (MSCRG). *Ann. Neurol. 39:285.*
4. Comi, G., M. Filippi, F. Barkhof, L. Durelli, G. Edan, O. Fernandez, H. Hartung, P. Seeldrayers, P. S. Sorensen, M. Rovaris, et al. 2001. Effect of early interferon treatment on conversion to definite multiple sclerosis: a randomised study. *Lancet 357:1576.*
5. Jacobs, L. D., R. W. Beck, J. H. Simon, R. P. Kinkel, C. M. Brownscheidle, T. J. Murray, N. A. Simonian, P. J. Slasor, and A. W. Sandrock. 2000. Intramuscular interferon β-1a therapy initiated during a first demyelinating event in multiple sclerosis. CHAMPS Study Group. *N. Engl. J. Med. 343:898.*
6. Gayo, A., L. Mozo, A. Suarez, A. Tunon, C. Lahoz, and C. Gutierrez. 1999. Interferon β-1b treatment modulates TNFα and IFNγ spontaneous gene expression in MS. *Neurology 52:1764.*
7. Rudick, R. A., R. M. Ransohoff, J. C. Lee, R. Peppler, M. Yu, P. M. Mathisen, and V. K. Tuohy. 1998. In vivo effects of interferon β-1a on immunosuppressive cytokines in multiple sclerosis [published erratum appears in Neurology 1998 Jul;51(1):332]. *Neurology 50:1294.*
8. Stone, L. A., J. A. Frank, P. S. Albert, C. N. Bash, P. A. Calabresi, H. Maloni, and H. F. McFarland. 1997. Characterization of MRI response to treatment with interferon β-1b: contrast-enhancing MRI lesion frequency as a primary outcome measure. *Neurology 49:862.*
9. Chomczynski, P. 1993. A reagent for the single-step simultaneous isolation of RNA, DNA and proteins from cell and tissue samples. *BioTechniques 15:532.*
10. Chomczynski, P., and K. Mackey. 1995. Short technical reports. Modification of the TRI reagent procedure for isolation of RNA from polysaccharide- and proteoglycan-rich sources. *BioTechniques 19:942.*
11. Ramoni, M. F., P. Sebastiani, and I. S. Kohane. 2002. Cluster analysis of gene expression dynamics. *Proc. Natl. Acad. Sci. USA 99:9121.*
12. Daido, H., M. Y. Zhou, E. P. Gomez-Sanchez, and C. E. Gomez-Sanchez. 2003. Interferon-inducible genes in the rat adrenal gland and vascular smooth muscle cells. *Mol. Cell. Endocrinol. 200:81.*

13. Pru, J. K., K. J. Austin, A. L. Haas, and T. R. Hansen. 2001. Pregnancy and interferon-tau upregulate gene expression of members of the 1–8 family in the bovine uterus. *Biol. Reprod. 65:1471*.
14. Bustin, S. A. 2000. Absolute quantification of mRNA using real-time reverse transcription polymerase chain reaction assays. *J. Mol. Endocrinol. 25:169*.
15. Der, S. D., A. Zhou, B. R. Williams, and R. H. Silverman. 1998. Identification of genes differentially regulated by interferon α, β, or γ using oligonucleotide arrays. *Proc. Natl. Acad. Sci. USA 95:15623*.
16. Stark, G. R., I. M. Kerr, B. R. Williams, R. H. Silverman, and R. D. Schreiber. 1998. How cells respond to interferons. *Annu. Rev. Biochem. 67:227*.
17. de Veer, M. J., M. Holko, M. Frevel, E. Walker, S. Der, J. M. Paranjape, R. H. Silverman, and B. R. Williams. 2001. Functional classification of interferon-stimulated genes identified using microarrays. *J. Leukocyte Biol. 69:912*.
18. Boehm, U., T. Klamp, M. Groot, and J. C. Howard. 1997. Cellular responses to interferon-γ. *Annu. Rev. Immunol. 15:749*.
19. Bertolotto, A., F. Gilli, A. Sala, L. Audano, A. Castello, U. Magliola, F. Melis, and M. T. Giordana. 2001. Evaluation of bioavailability of three types of IFNβ in multiple sclerosis patients by a new quantitative-competitive-PCR method for MxA quantification. *J. Immunol. Methods 256:141*.
20. Salmon, P., J. Y. Le Cotonnec, A. Galazka, A. Abdul-Ahad, and A. Darragh. 1996. Pharmacokinetics and pharmacodynamics of recombinant human interferon-β in healthy male volunteers. *J. Interferon Cytokine Res. 16:759*.
21. Buchwalder, P. A., T. Buclin, I. Trinchard, A. Munafo, and J. Biollaz. 2000. Pharmacokinetics and pharmacodynamics of IFN-β 1a in healthy volunteers. *J. Interferon Cytokine Res. 20:857*.
22. Fierlbeck, G., A. Ulmer, T. Schreiner, W. Stroebel, U. Schiebel, and J. Brzoska. 1996. Pharmacodynamics of recombinant IFN-β during long-term treatment of malignant melanoma. *J. Interferon Cytokine Res. 16:777*.
23. Whitney, L. W., K. G. Becker, N. J. Tresser, C. I. Caballero-Ramos, P. J. Munson, V. V. Prabhu, J. M. Trent, H. F. McFarland, and W. E. Biddison. 1999. Analysis of gene expression in mutiple sclerosis lesions using cDNA microarrays. *Ann. Neurol. 46:425*.
24. Lock, C., G. Hermans, R. Pedotti, A. Brendolan, E. Schadt, H. Garren, A. Langer-Gould, S. Strober, B. Cannella, J. Allard, et al. 2002. Gene-microarray analysis of multiple sclerosis lesions yields new targets validated in autoimmune encephalomyelitis. *Nat. Med. 8:500*.
25. Whitney, L. W., S. K. Ludwin, H. F. McFarland, and W. E. Biddison. 2001. Microarray analysis of gene expression in multiple sclerosis and EAE identifies 5-lipoxygenase as a component of inflammatory lesions. *J. Neuroimmunol. 121:40*.
26. Chabas, D., S. E. Baranzini, D. Mitchell, C. C. Bernard, S. R. Rittling, D. T. Denhardt, R. A. Sobel, C. Lock, M. Karpuj, R. Pedotti, et al. 2001. The influence of the proinflammatory cytokine, osteopontin, on autoimmune demyelinating disease. *Science 294:1731*.
27. Wandinger, K. P., C. S. Sturzebecher, B. Bielekova, G. Detore, A. Rosenwald, L. M. Staudt, H. F. McFarland, and R. Martin. 2001. Complex immunomodulatory effects of interferon-β in multiple sclerosis include the upregulation of T helper 1-associated marker genes. *Ann. Neurol. 50:349*.
28. Satoh, J., and Y. Kuroda. 2001. Differing effects of IFN β vs IFN γ in MS: gene expression in cultured astrocytes. *Neurology 57:681*.
29. Boehm, U., L. Guethlein, T. Klamp, K. Ozbek, A. Schaub, A. Futterer, K. Pfeffer, and J. C. Howard. 1998. Two families of GTPases dominate the complex cellular response to IFN-γ. *J. Immunol. 161:6715*.
30. Hartrich, L., B. Weinstock-Guttman, D. Hall, D. Badgett, M. Baier, K. Patrick, J. Feichter, J. Hong, and M. Ramanathan. 2003. Dynamics of immune cell trafficking in interferon-β treated multiple sclerosis patients. *J. Neuroimmunol. 139:84*.
31. Comabella, M., K. Balashov, S. Issazadeh, D. Smith, H. L. Weiner, and S. J. Khoury. 1998. Elevated interleukin-12 in progressive multiple sclerosis correlates with disease activity and is normalized by pulse cyclophosphamide therapy. *J. Clin. Invest. 102:671*.
32. Galboiz, Y., S. Shapiro, N. Lahat, and A. Miller. 2002. Modulation of monocytes matrix metalloproteinase-2, MT1-MMP and TIMP-2 by interferon-γ and -β: implications to multiple sclerosis. *J. Neuroimmunol. 131:191*.
33. Floris, S., S. R. Ruuls, A. Wierinckx, S. M. van der Pol, E. Dopp, P. H. van der Meide, C. D. Dijkstra, and H. E. De Vries. 2002. Interferon-β directly influences monocyte infiltration into the central nervous system. *J. Neuroimmunol. 127:69*.
34. Comabella, M., J. Imitola, H. L. Weiner, and S. J. Khoury. 2002. Interferon-β treatment alters peripheral blood monocytes chemokine production in MS patients. *J. Neuroimmunol. 126:205*.
35. Baranzini, S. E., and S. L. Hauser. 2002. Large-scale gene-expression studies and the challenge of multiple sclerosis. *Genome Biol. 3:1027*.
36. Oksenberg, J. R., L. F. Barcellos, and S. L. Hauser. 1999. Genetic aspects of multiple sclerosis. *Semin. Neurol. 19:281*.
37. Prat, E., and R. Martin. 2002. The immunopathogenesis of multiple sclerosis. *J. Rehabil. Res. Dev. 39:187*.
38. Tompkins, S. M., and S. D. Miller. 2002. An array of possibilities for multiple sclerosis. *Nat. Med. 8:451*.
39. Steinman, L. 2001. Gene microarrays and experimental demyelinating disease: a tool to enhance serendipity. *Brain 124:1897*.